Figure 2.7 Necktie clip portion. The necktie-mounted visual augmented reality system. A smoked plexiglass dome of wine-dark opacity is used to conceal the inner components. Wiring from these components to a body-concealed computer runs through the crack in the front of the shirt. The necktie helps conceal the wiring.

2.6 PORTABLE PERSONAL PULSE DOPPLER RADAR VISION SYSTEM BASED ON TIME–FREQUENCY ANALYSIS AND *q*-CHIRPLET TRANSFORM

> "Today we saw Mary Baker Eddy with one eye!" — a deliberately cryptic sentence inserted into a commercial shortwave broadcast to secretly inform colleagues across the Atlantic of the successful radar imaging of a building (spire of Christian Science building; Mary Baker Eddy, founder) with just one antenna for both receiving and transmitting. Prior to this time, radar systems required two separate antennas, one to transmit, and the other to receive.

Telepointer, the necktie worn dome ("tiedome") of the previous section bears a great similarity to radar, and how radar in general works. In many ways the telepointer tiedome is quite similar to the radomes used for radar antennas. The telepointer was a front-facing two-way imaging apparatus. We now consider a backward-facing imaging apparatus built into a dome that is worn on the back.

Time–frequency and q-chirplet-based signal processing is applied to data from a small portable battery-operated pulse Doppler radar vision system designed and built by the author. The radar system and computer are housed in a miniature radome backpack together with video cameras operating in various spectral bands, to be backward-looking, like an eye in the back of the head. Therefore all the ground clutter is moving away from the radar when the user walks forward, and is easy to ignore because the radar has separate in-phase and quadrature channels that allow it to distinguish between negative and positive Doppler. A small portable battery powered computer built into the miniature radome allows the entire system to be operated while attached to the user's body. The fundamental hypothesis upon which the system operates is that actions such as an attack or pickpocket by someone sneaking up behind the user, or an automobile on a collision course from behind the user, are governed by accelerational

intentionality. Intentionality can change abruptly and gives rise to application of roughly constant force against constant mass. Thus the physical dynamics of most situations lead to piecewise uniform acceleration, for which the Doppler returns are piecewise quadratic chirps. These q-chirps are observable as peaks in the q-chirplet transform [28].

2.6.1 Radar Vision: Background, Previous Work

Haykin coined the term "radar vision" in the context of applying methodology of machine vision to radar systems [5]. Traditionally radar systems were not coherent, but recent advances have made the designing and building of coherent radar systems possible [25]. Coherent radar systems, especially when having separate in-phase and quadrature components (e.g., providing a complex-valued output), are particularly well suited to Doppler radar signal processing [26] (e.g., see Fig. 2.8). Time–frequency analysis makes an implicit assumption of short-time stationarity, which, in the context of Doppler radar, is isomorphic to an assumption of short-time constant velocity. Thus the underlying assumption is that the velocity is piecewise constant. This assumption is preferable to simply taking a Fourier transform over the entire data record, but we can do better by modeling the underlying physical phenomena.

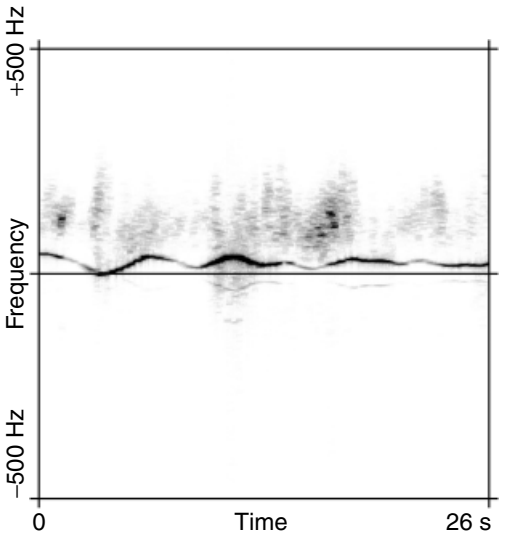

Figure 2.8 Sliding window Fourier transform of small but dangerous floating iceberg fragment as seen by an experimental pulse Doppler X-band marine radar system having separate in-phase and quadrature components. The radar output is a complex-valued signal for which we can distinguish between positive and negative frequencies. The chosen window comprises a family of discrete prolate spheroidal sequences [27]. The unique sinusoidally varying frequency signature of iceberg fragments gave rise to the formulation of the w-chirplet transform [28]. Safer navigation of oceangoing vessels was thus made possible.

Instead of simply using sines and cosines, as in traditional Fourier analysis, sets of parameterized functions are now often used for signal analysis and representation. The wavelet transform [29,30] is one such example having parameters of time and scale. The chirplet transform [28,31,32,33] has recently emerged as a new kind of signal representation. Chirplets include sets of parameterized signals having polynomial phase (piecewise cubic, piecewise quadratic, etc.) [28], sinusoidally varying phase, and projectively varying periodicity. Each kind of chirplet is optimized for a particular problem. For example, warbling chirplets (w-chirplets), also known as warblets [28], were designed for processing Doppler returns from floating iceberg fragments that bob around in a sinusoidal manner as seen in Figure 2.8. The sinusoidally varying phase of the w-chirplet matches the sinusoidally varying motion of iceberg fragments driven by ocean waves.

Of all the different kinds of chirplets, it will be argued that the q-chirplets (quadratic phase chirplets) are the best suited to processing of Doppler returns from land-based radar where accelerational intentionality is assumed. Q-chirplets are based on q-chirps (also called "linear FM"), $\exp(2\pi i(a + bt + ct^2))$ with phase a, frequency b, and chirpiness c. The Gaussian q-chirplet,

$$\psi_{t_0,b,c,\sigma} = \frac{1}{\sqrt{2\pi}\sigma} \exp\left(2\pi i(a + bt_c + ct_c^2) - \frac{1}{2}\left(\frac{t_c}{\sigma}\right)^2\right) \Big/ \sqrt{2\pi\sigma}$$

is a common form of q-chirplet [28], where $t_c = t - t_0$ is a movable time axis. There are four meaningful parameters, phase a being of lesser interest when looking at the magnitude of

$$\langle \psi_{t_0,b,c,\sigma} | z(t) \rangle \tag{2.1}$$

which is the q-chirplet transform of signal $z(t)$ taken with a Gaussian window. Q-chirplets are also related to the fractional Fourier transform [34].

2.6.2 Apparatus, Method, and Experiments

Variations of the apparatus to be described were originally designed and built by the author for assisting the blind. However, the apparatus has many uses beyond use by the blind or visually challenged. For example, we are all blind to objects and hazards that are behind us, since we only have eyes in the forward-looking portion of our heads.

A key assumption is that objects in front of us deserve our undivided attention, whereas objects behind us only require attention at certain times when there is a threat. Thus an important aspect of the apparatus is an intelligent rearview system that alerts us when there is danger lurking behind us, but otherwise does not distract us from what is in front of us. Unlike a rearview mirror on a helmet (or a miniature rearview camera with eyeglass-based display), the radar vision system is an intelligent system that provides us with timely information only when needed, so that we do not suffer from information overload.

Rearview Clutter is Negative Doppler

A key inventive step is the use of a rearview radar system whereby ground clutter is moving away from the radar while the user is going forward. This rearview configuration comprises a backpack in which the radome is behind the user and facing backward.

This experimental apparatus was designed and built by the author in the mid-1980s, from low-power components for portable battery-powered operation. A variation of the apparatus, having several sensing instruments, including radar, and camera systems operating in various spectral bands, including infrared, is shown in Figure 2.9. The radome is also optically transmissive in the visible and infrared. A general description of radomes may be found in `http://www.radome.net/`, although the emphasis has traditionally been on

Figure 2.9 Early personal safety device (PSD) with radar vision system designed and built by the author, as pictured on exhibit at List Visual Arts Center, Cambridge, MA (October 1997). The system contains several sensing instruments, including radar, and camera systems operating in various spectral bands, including infrared. The headworn viewfinder display shows what is behind the user when targets of interest or concern appear from behind. The experience of using the apparatus is perhaps somewhat like having eyes in the back of the head, but with extra signal processing as the machine functions like an extension of the brain to provide visual intelligence. As a result the user experiences a sixth or seventh sense as a radar vision system. The antenna on the hat was for an early wireless Internet connection allowing multiple users to communicate with each other and with remote base stations.

radomes the size of a large building rather than in sizes meant for a battery-operated portable system.

Note that the museum artifact pictured in Figure 2.9 is a very crude early embodiment of the system. The author has since designed and built many newer systems that are now so small that they are almost completely invisible.

On the Physical Rationale for the q-Chirplet

The apparatus is meant to detect persons such as stalkers, attackers, assailants, or pickpockets sneaking up behind the user, or to detect hazardous situations, such as arising from drunk drivers or other vehicular traffic notations.

It is assumed that attackers, assailants, pickpockets, as well as ordinary pedestrian, bicycle, and vehicular traffic, are governed by a principle of accelerational intentionality. The principle of accelerational intentionality means that an individual attacker (or a vehicle driven by an individual person) is governed by a fixed degree of acceleration that is changed instantaneously and held roughly constant over a certain time interval. For example, an assailant is capable of a certain degree of exertion defined by the person's degree of fitness

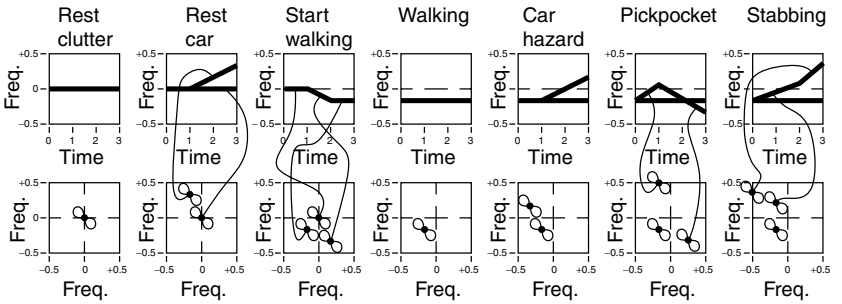

Figure 2.10 Seven examples illustrating the principle of accelerational intentionality, with time-frequency distribution shown at top, and corresponding chirplet transform frequency–frequency distribution below. REST CLUTTER: Radar return when the author (wearing the radar) is standing still. REST CAR: A car parked behind the author is set in motion when its driver steps on the accelerator; a roughly constant force of the engine is exerted against the constant mass of the car while the author (wearing the radar) is standing still. START WALKING: The author stands still for one second, and then decides to start walking. The decision to start walking is instantaneous, but the human body applies a roughly constant degree of force to its constant mass, causing it to accelerate until it reaches the desired walking speed. This takes approximately 1 second. Finally the author walks at this speed for another one second. All of the clutter behind the author (ground, buildings, lamp posts, etc.) is moving away from the author, so it moves into negative frequencies. WALKING: At a constant pace all of the clutter has a constant (negative) frequency. CAR HAZARD: While the author is walking forward, a parked car is switched into gear at time 1 second. It accelerates toward the author. The system detects this situation as a possible hazard, and brings an image up on the screen. PICKPOCKET: Rare but unique radar signature of a person lunging up behind the author and then suddenly switching to a decelerating mode (at time 1 second), causing reduction in velocity to match that of the author (at time 2 seconds) followed by a retreat away from the author. STABBING: Acceleration of attacker's body toward author, followed by a swing of the arm (initiated at time 2 seconds) toward the author.

which is unlikely to change over the short time period of an attack. The instant the attacker spots a wallet in a victim's back pocket, the attacker may accelerate by applying a roughly constant force (defined by his fixed degree of physical fitness) against the constant mass of the attacker's own body. This gives rise to uniform acceleration which shows up as a straight line in the time–frequency distribution.

Some examples following the principle of accelerational intentionality are illustrated in Figure 2.10.

Examples of Chirplet Transforms of Radar Data

A typical example of a radar data test set, comprising half a second (4,000 points) of radar data (starting from $t = 1.5$ seconds and running to $t = 2$ seconds in the "car3E" dataset) is shown in Figure 2.11. Here we see a two-dimensional slice known as frequency–frequency analysis [28] taken through the chirplet

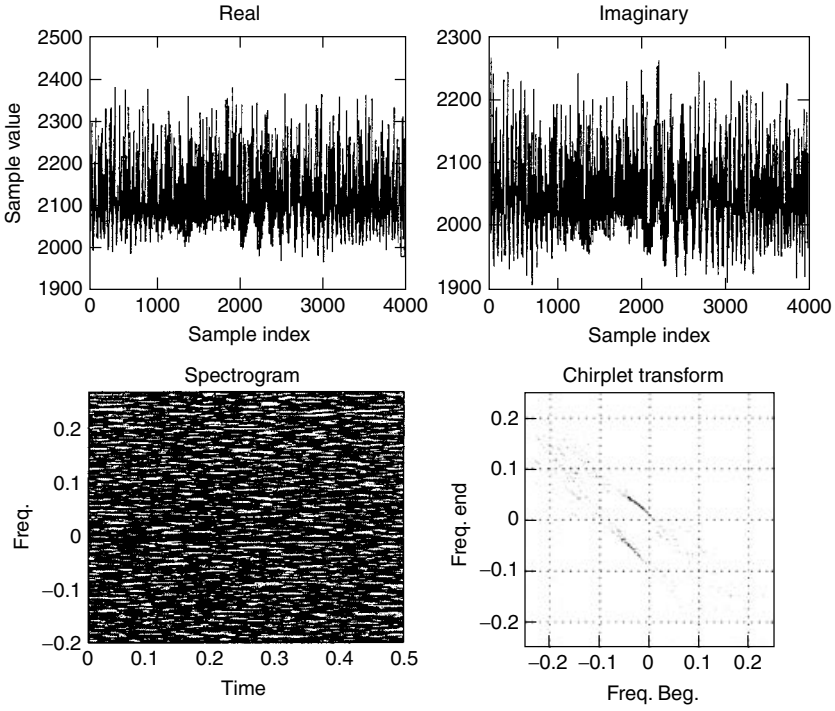

Figure 2.11 Most radar systems do not provide separate real and imaginary components and therefore cannot distinguish between positive and negative frequencies (e.g., whether an object is moving toward the radar or going away from it). The author's radar system provides in-phase and quadrature components: REAL and IMAG (imaginary) plots for 4,000 points (half a second) of radar data are shown. The author was walking at a brisk pace, while a car was accelerating toward the author. From the time–frequency distribution of these data we see the ground clutter moving away and the car accelerating toward the author. The chirplet transform shows two distinct peaks, one corresponding to all of the ground clutter (which is all moving away at the same speed) and the other corresponding to the accelerating car.

transform, in which the window size σ is kept constant, and the time origin t_0 is also kept constant. The two degrees of freedom of frequency b and chirpiness c are parameterized in terms of instantaneous frequency at the beginning and end of the data record, to satisfy the Nyquist chirplet criterion [28]. Here we see a peak for each of the two targets: the ground clutter (e.g., the whole world) moving away; and the car accelerating toward the radar. Other examples of chirplet transforms from the miniature radar set are shown in Figure 2.12.

Calibration of the Radar

The radar is a crude home-built system, operating at approximately 24 gigahertz, and having an interface to an Industry Standards Association (ISA) bus. Due to the high frequency involved, such a system is difficult to calibrate perfectly, or even closely. Thus there is a good deal of distortion, such as mirroring in the FREQ $= 0$ axis, as shown in Figure 2.13. Once the radar was calibrated, data could be analyzed with surprising accuracy, despite the crude and simple construction of the apparatus.

Experimental Results

Radar targets were classified based on their q-chirplet transforms, with approximately 90% accuracy, using the mathematical framework and methods described in [28] and [35]. Some examples of the radar data are shown as time–frequency distributions in Figure 2.14.

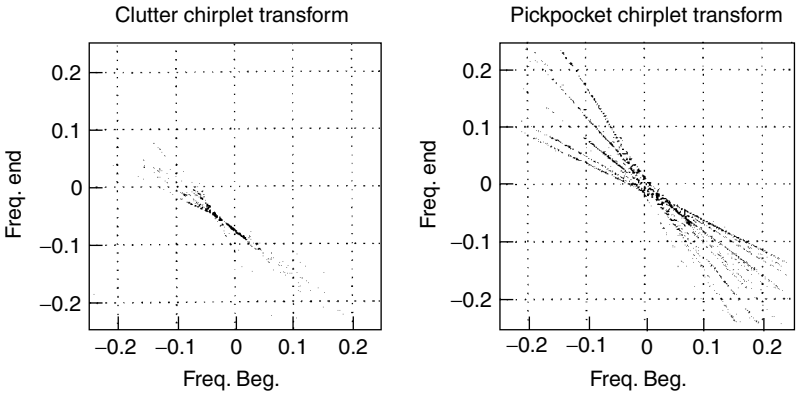

Figure 2.12 Chirplet transforms for ground clutter only, and pickpocket only. Ground clutter falls in the lower left quadrant because it is moving away from the radar at both the beginning and end of any time record (window). Note that the pickpocket is the only kind of activity that appears in the lower right-hand quadrant of the chirplet transform. Whenever there is any substantial energy content in this quadrant, we can be very certain there is a pickpocket present.

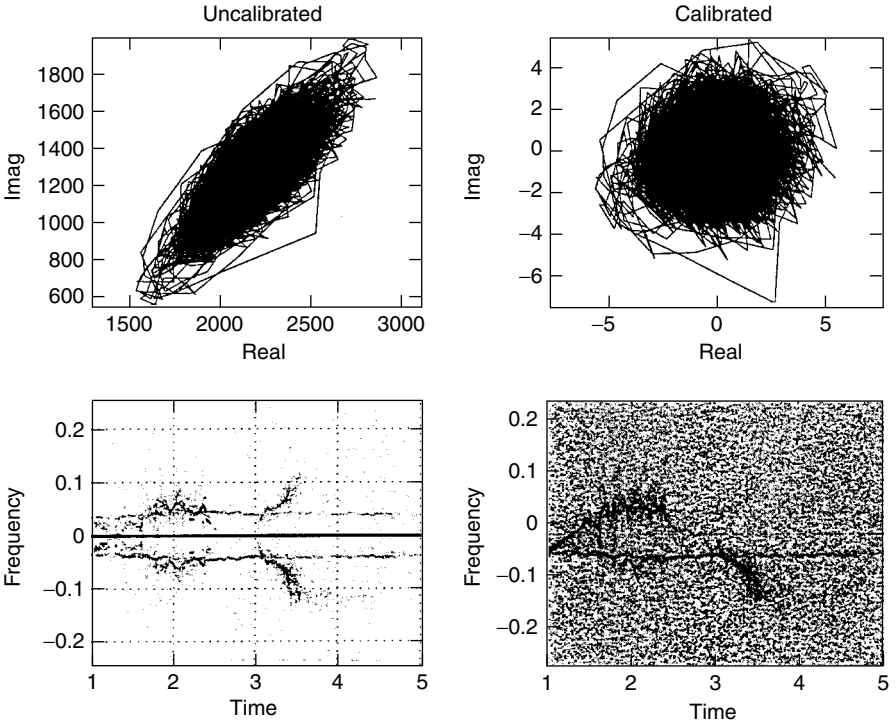

Figure 2.13 The author's home-built radar generates a great deal of distortion. Notice, for example, that a plot of real versus imaginary data shows a strong correlation between real and imaginary axes, and also an unequal gain in the real and imaginary axes, respectively (note that the unequal signal strength of REAL and IMAG returns in the previous figure as well). Note further that the dc offset gives rise to a strong signal at $f = 0$, even though there was nothing moving at exactly the same speed as the author (e.g., nothing that could have given rise to a strong signal at $f = 0$). Rather than trying to calibrate the radar exactly, and to remove dc offset in the circuits (all circuits were dc coupled), and risk losing low-frequency components, the author mitigated these problems by applying a calibration program to the data. This procedure subtracted the dc offset inherent in the system, and computed the inverse of the complex Choleski factorization of the covariance matrix (e.g., covz defined as covariance of real and imaginary parts), which was then applied to the data. Notice how the CALIBRATED data forms an approximately isotropic circular blob centered at the origin when plotted as REAL versus IMAGinary. Notice also the removal of the mirroring in the FREQ = 0 axis in the CALIBRATED data, which was quite strong in the UNCALIBRATED data.

2.7 WHEN BOTH CAMERA AND DISPLAY ARE HEADWORN: PERSONAL IMAGING AND MEDIATED REALITY

When both the image acquisition and image display embody a headworn first-person perspective (e.g., computer takes input from a headworn camera and provides output to a headworn display), a new and useful kind of experience results, beyond merely augmenting the real world with a virtual world.

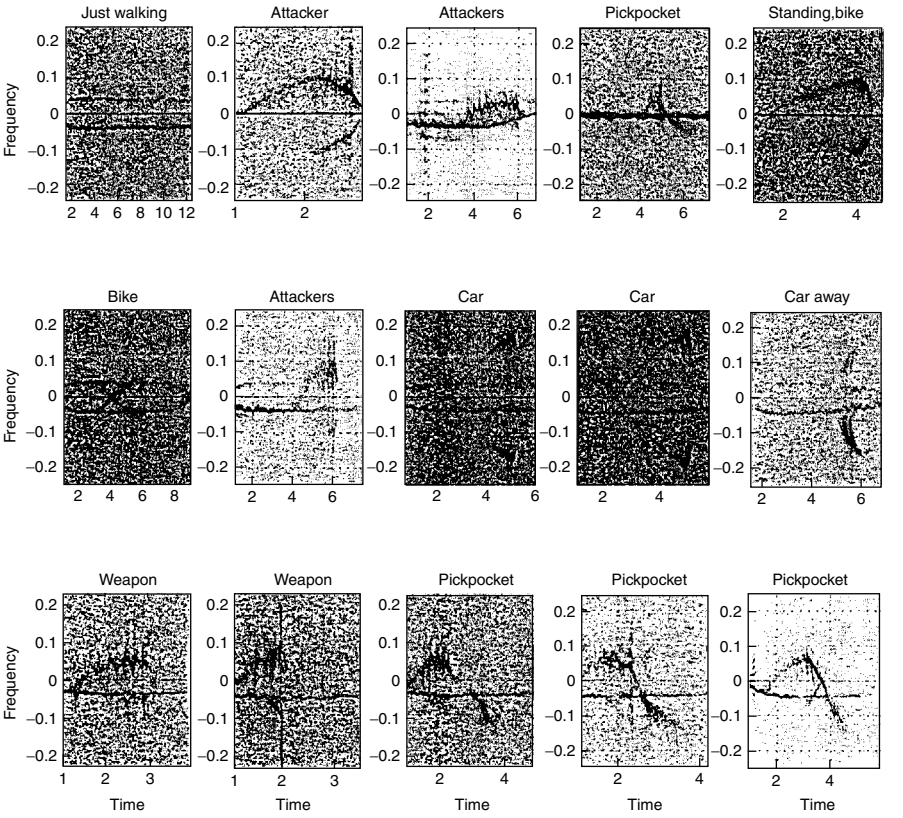

Figure 2.14 Various test scenarios were designed in which volunteers carried metal objects to simulate weapons, or lunged toward the author with pieces of metal to simulate an attack. Pickpockets were simulated by having volunteers sneak up behind the author and then retreat. The ''pickpocket signature'' is a unique radar signature in which the beginning and ending frequency fall on either side of the frequency defined by author's walking Doppler frequency. It was found that of all the radar signatures, the pickpocket signature was the most unique, and easiest to classify. The car plot in the middle of the array of plots was misclassified as a stabbing. It appears the driver stepped on the accelerator lightly at about time 1 second. Then just before time 3 seconds it appears that the driver had a sudden change of intentionality (perhaps suddenly realized lateness, or perhaps suddenly saw that the coast was clear) and stepped further on the accelerator, giving rise to an acceleration signature having two distinct portions.